

锯齿形细通道内乙醇流动沸腾特性研究

常 威 张树生 郭 雷

(山东大学 能源与动力工程学院, 山东 济南 250061)

摘 要: 采用数值模拟的方法对通道宽度为 2 mm 的竖直布置的锯齿形细通道内乙醇流动沸腾及传热特性展开研究。通过 UDF 编程的方法对相界面的传热传质过程进行控制, 重点考察了气泡的生长特性及其对系统压差和换热系数的影响。结果表明: 锯齿形细通道内起始汽化核心均位于内侧突起点附近, 且在漂移区和泡底微层共同作用下, 该区域工质平均流速高达主流流速的 5~10 倍, 使得该处的气泡生长速度最快, 换热增强。系统压差随加热时间呈上升趋势, 并在一定范围内震荡。传热系数随干度增大而下降, 并将模拟结果与实验数据进行了对比分析, 阐述了流型和通道几何结构对于传热系数的影响。

关 键 词: 锯齿形细通道; 强化传热; 乙醇; 数值模拟

中图分类号: TK124 文献标识码: A

引 言

20 世纪 60 年代, Ishibashi 等人就在一组横向对比试验中发现当流道间隙小于 3 mm 时, 沸腾换热现象得到明显的强化^[1]。Tuckerman 等人对于水流过微管槽道的实验研究也表明, 减小槽道的水力直径可显著增加水的对流换热系数^[2]。Fukano 等人对内径分别为 1、2.4 和 4.9 mm 的细圆管内气-水两相流动的实验研究中发现, 在大尺度通道中可忽略的表面张力是影响微细通道内两相流流型的重要因素^[3]。近期的一些研究结果也验证了这一结论^[4-6]。

就现有文献来看, 对这一课题的研究还处在探索阶段, 研究者多采用实验的方法来进行研究。为了克服实验条件要求苛刻, 实验可重复性差等缺点, 本研究利用数值模拟的方法, 选取乙醇作为工质, 借助于商用 CFD 软件, 通过 UDF 编程的方法, 对所建立的二维细通道模型内的乙醇沸腾流动及传热特性进行探索。

1 数值模拟

1.1 模型建立

建立如图 1 所示的二维几何模型用于本研究的数值模拟。细通道竖直布置, 工质由下至上流经细通道。通道进出口宽度均为 2 mm, 总长 100 mm, 单一锯齿单元长度 l 为 4 mm, 左右两侧锯齿形壁面为加热面。

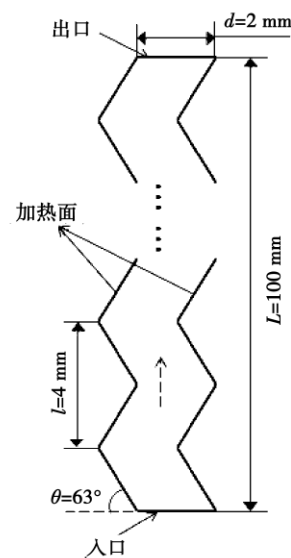


图 1 锯齿形细通道结构示意图

Fig. 1 Structural schematic drawing of a serrated slim passage

1.2 相界面处理

利用 CFD 数值模拟软件内 UDF 函数对气液相间相互转化的质量和相变潜热进行了定义:

当 $T \geq T_{\text{sat}}$ (沸腾状态),

收稿日期: 2011-05-24; 修订日期: 2011-06-28

基金项目: 国家重点基础研究发展计划(973 计划) 基金资助项目(2007CB206900)

作者简介: 常 威(1984-), 男, 河北秦皇岛人, 山东大学博士研究生.

$$R_l = -\lambda\alpha_l\rho_l \frac{|T - T_{sat}|}{T_{sat}} \quad R_v = \lambda\alpha_v\rho_v \frac{|T - T_{sat}|}{T_{sat}}$$

当 $T < T_{sat}$ (凝结状态) ,

$$R_l = \lambda\alpha_v\rho_v \frac{|T - T_{sat}|}{T_{sat}} \quad R_v = -\lambda\alpha_l\rho_l \frac{|T - T_{sat}|}{T_{sat}}$$

式中: α_v, α_l —气相和液相体积分数; $\alpha_v + \alpha_l = 1$; ρ_v, ρ_l —气相和液相的密度, kg/m^3 ; R_v, R_l —相间传质, $\text{kg}/\text{m}^3 \cdot \text{s}^{-1}$; T —系统温度, K ; T_{sat} —饱和温度, K ; λ —松弛因子 s^{-1} 。

由于细通道沸腾换热时间短、加热迅速且气泡对流动扰动较强,工质在很短时间内即可发生相态变化,因此选取较小的松弛因子进行迭代计算,其取值范围在 0.1~0.3 之间,并根据残差变化情况对其进行及时调整,在保证收敛的前提下,尽量提高松弛因子以加快收敛速度。

界面处的传热量计算为:

$$q = m \times h_{fg}$$

式中: m —气液间相互转化的质量, kg ; h_{fg} —汽化潜热, J/kg 。

由于表面张力对工质在微细通道内的流动沸腾有着重要影响,因此对表面张力进行了变物性处理。将乙醇表面张力与温度的关系式通过 C 语言编程写入 UDF 中,通过在数值模拟中调用编译该 UDF 程序来实现表面张力的变物性控制。程序中设定乙醇表面张力与温度的关系:

$$\sigma = 131.38 \times (1 - T)^{5.5437 - 8.4826T + 4.3164T^2}$$

细通道内乙醇流动的克努森数小于 0.001,故采用无滑移条件的 $N - S$ 方程进行计算。

气相动量方程为:

$$\frac{\partial}{\partial t}(\alpha_v\rho_v V_v) + \nabla \cdot (\alpha_v\rho_v V_v V_v) = -\nabla \cdot (\alpha_v P) +$$

$$\nabla \cdot [\mu'_{eff,v}(\nabla V_v + \nabla V_v^T)] + F_{d,v} + \Gamma_{lv}V_l + \alpha_v\rho_v g$$

液相动量方程为:

$$\frac{\partial}{\partial t}(\alpha_l\rho_l V_l) + \nabla \cdot (\alpha_l\rho_l V_l V_l) = -\nabla \cdot (\alpha_l P) +$$

$$\nabla \cdot [\mu'_{eff,l}(\nabla V_l + \nabla V_l^T)] + F_{d,l} + \Gamma_{vl}V_v + \alpha_l\rho_l g$$

式中: μ'_{eff} —有效粘度, $\text{Pa} \cdot \text{s}$; V_v, V_l —气、液相沿流动方向的速度, m/s ; V_v^T, V_l^T —气、液相沿截面方向的速度分量, m/s ; P —运行压力, Pa ; g —重力加速度, m/s^2 ; $F_{d,v}, F_{d,l}$ —分别表示气相对液相、液相对气相所施加的拖曳力, N ,具体计算方法参考文献 [7]。

传热和传质过程同时存在于乙醇沸腾的气液界面上。

界面处气相质量守恒方程:

$$\frac{\partial}{\partial t}(\alpha_v\rho_v) + \nabla \cdot (\alpha_v\rho_v V_v) = \nabla \cdot (\rho_v D_v \nabla \alpha_v) + \Gamma_{lv}$$

界面处液相质量守恒方程:

$$\frac{\partial}{\partial t}(\alpha_l\rho_l) + \nabla \cdot (\alpha_l\rho_l V_l) = \nabla \cdot (\rho_l D_l \nabla \alpha_l) + \Gamma_{vl}$$

式中: D —与相的有效粘度相等的扩散系数, m^2/s 。

蒸发或冷凝速率 Γ_{lv} 为 [8]:

$$\Gamma_{lv} = \frac{h_{lv}A_{lv}(T_{sat} - T_l)}{h_{fg}} \quad \Gamma_{vl} = \frac{h_{lv}A_{lv}(T_l - T_{sat})}{h_{fg}}$$

式中: h_{lv} —相间换热系数, $\text{W}/(\text{m}^2 \cdot \text{K})$; A_{lv} —单元体积的界面面积, m^{-1} 。

单元体积的界面面积 A_{lv} 与气相体积分数 α_v 和气泡直径 d_b (m) 有关:

$$A_{lv} = 6\alpha_v/d_b$$

其中气泡直径 d_b 为:

$$d_b = 0.5d_{max}$$

式中: d_{max} —根据临界韦伯数 (We_{crit}) 估计的气泡最大直径, $d_{max} = \frac{\sigma We_{crit}}{\rho_l (V_l - V_g)^2}$, m ,对于泡状流,可以假设临界韦伯数为 10 来估算最大气泡直径。

在相界面上,假设液相和气相均为不可压缩流体,压力对时间的倒数可以忽略,气相能量方程为:

$$\frac{\partial}{\partial t}(\alpha_v\rho_v c_{pv} T_v) + \nabla \cdot (\alpha_v\rho_v c_{pv} V_v T_v) = \nabla \cdot (k'_v \nabla T_v) + q_{lv} + \Gamma_{lv}h_l$$

$$= \nabla \cdot (k'_v \nabla T_v) + q_{lv} + \Gamma_{lv}h_l$$

液相能量方程为:

$$\frac{\partial}{\partial t}(\alpha_l\rho_l c_{pl} T_l) + \nabla \cdot (\alpha_l\rho_l c_{pl} V_l T_l) = \nabla \cdot (k'_l \nabla T_l) + q_{vl} + \Gamma_{vl}h_v$$

$$= \nabla \cdot (k'_l \nabla T_l) + q_{vl} + \Gamma_{vl}h_v$$

式中: C_{pv}, C_{pl} —气、液相的定压比热容, $\text{J}/(\text{kg} \cdot \text{K})$; T_v, T_l —气、液相的温度, K ; k'_v, k'_l —气、液相有效导热系数, $\text{W}/(\text{m} \cdot \text{K})$; q_{lv}, q_{vl} —气液两相转化所需要的能量, J ; h_l —液相的焓, J ; h_v —气相的焓, J 。

1.3 求解方法

选用 VOF 模型对乙醇在细通道流动沸腾过程中气泡的产生、生长和脱离过程进行数值模拟,通过求解两相比率方程获得气、液相边界的位置。VOF 模型引入计算单元的相体积分数 α ,气相和液相的体积分数分别为 α_v 和 α_l 。当 $\alpha_v = 1$ 时为气相区域,当 $\alpha_l = 1$ 时为液相区域。对于各气泡的边界,即气-液共存的分界面,则 α_v 和 α_l 在 0~1 之间,由此可确定气泡边界。通过几何重构的方式,VOF 模型获取气液相分界面的几何信息,并由此计算两相流体的流量 [10]。

1.4 边界条件

软件中对于各求解选项的参数设置请参见文献

[9]。模拟过程中采用两竖直壁面作为加热面,采用恒定热流加热方式,设定上部出口的气相回流温度为351 K。设定初始系统温度为350 K,UDF中设定沸腾温度为351.6 K,且气泡从壁面处产生。数值模拟中取壁面粗糙度为定值,消除了实验中壁面粗糙度难于测定造成的影响。

2 结果和讨论

2.1 锯齿形细通道内乙醇沸腾的气泡生长特性

与常规通道相比,细通道内的工质沸腾换热所需加热时间短,沸腾迅速。实验研究中往往需要借助高速摄像设备才能捕捉到气泡产生、生长和脱离的过程。本研究利用数值模拟中时间步长可控的特点,实现了对这一过程的准确监测。

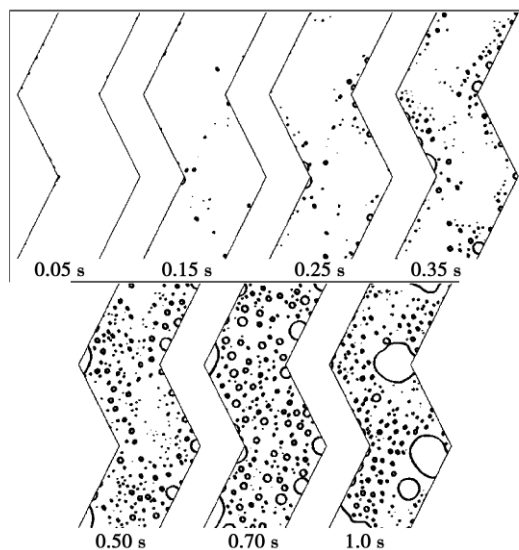


图2 锯齿形细通道内乙醇沸腾的气泡生长特性
Fig. 2 Bubble growth characteristics of ethanol during its boiling process inside a serrated slim passage

锯齿形细通道内乙醇沸腾的气泡生长特性如图2所示。加热开始后的0.05 s壁面过热到能有气相产生,此时远离壁面的主流温度仍处于过冷状态,有些细小的气泡产生后又消失掉。0.15~0.35 s壁面附近的液体已经全部过热,过热层向通道内部扩张,气泡持续增多,有些较大的气泡被主流携带从而脱离壁面,从0.15~0.35 s的3幅图中可以看出,气泡的起始成核部位均位于锯齿形细通道内侧突起点附近,且该处的气泡生长速度最快。0.35 s时,锯齿形细通道内侧突起点附近的气泡已经明显大于其它区域的气泡。0.35~0.7 s,脱离的以及壁面上的气泡

不断合并,形成较大的气泡,但此时气泡尺寸相对于通道尺寸仍然较小。加热1.0 s后,气泡继续合并,并形成很大的气泡,且其尺寸已经与通道尺寸处于同一个数量级。

2.2 成核起始点分析

由于锯齿形细通道自身结构的特殊性,其汽化核心的起始点分布也与常规通道有所不同。锯齿形细通道内起始汽化核心均位于内侧突起点附近,且该处的气泡生长速度最快。由图3的速度矢量图可看出,锯齿形细通道向内侧的突起对由下至上的主流流动起到了较强的扰动作用。这种扰动所影响的区域是以气泡核为中心,两倍于气泡直径的区域,被扰动的液体产生了平移、旋转和振动。郭雷等人在研究中也发现了类似区域,并称之为漂移区^[9]。该区域的存在将过热液体推向主流,在来流速度的影响下,过热液体的速度方向又发生了改变。不仅如此,成核区与壁面之间还存在着泡底微层。泡底微层沿壁面与主流方向相反的方向流入成核区域,且泡底微层作用区内工质的平均流速可达到主流流速的5~10倍。漂移区和泡底微层的共同作用,对锯齿形细通道内侧突起附近工质流动造成了剧烈的扰动,使得换热系数增大,气泡得以快速生长。

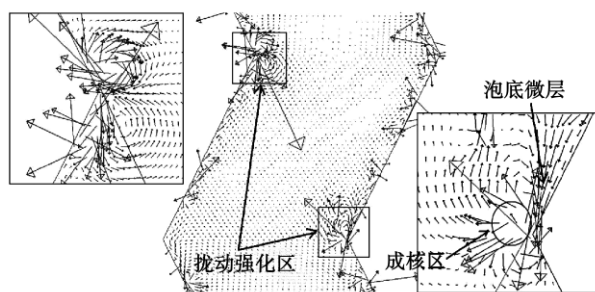


图3 锯齿型细通道内工质流动速度矢量图(0.15秒时刻)

Fig. 3 Flow speed vector chart of the working medium inside a serrated slim passage (at 0.15 seconds)

2.3 传热系数和系统压降

锯齿形细通道内乙醇沸腾过程的系统压差变化如图4所示。自加热开始后,整个系统压差呈上升趋势。0.15 s左右,随着过冷沸腾的出现,很小的气泡不断生成与消失,引起系统压差的小幅波动。0.35 s左右,气泡持续增多并长大,系统压差进一步增大。随着系统温度的进一步上升,气泡不断生成长大并融合,形成与通道尺寸同一数量级的大气泡,

最终脱离壁面。这些运动过程对整个系统产生了巨大的扰动,最终导致了压差的大幅度波动,并呈现出如图所示的振荡。

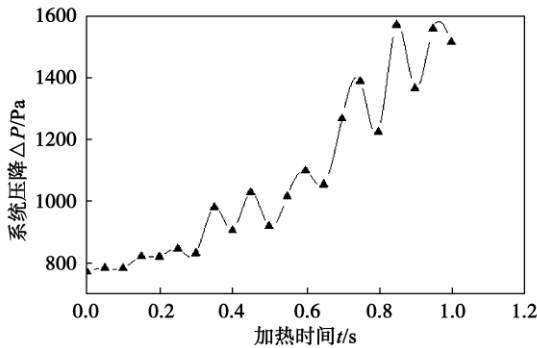


图 4 系统压差与加热时间的关系

Fig. 4 Relationship between the systematic pressure difference and the heating time

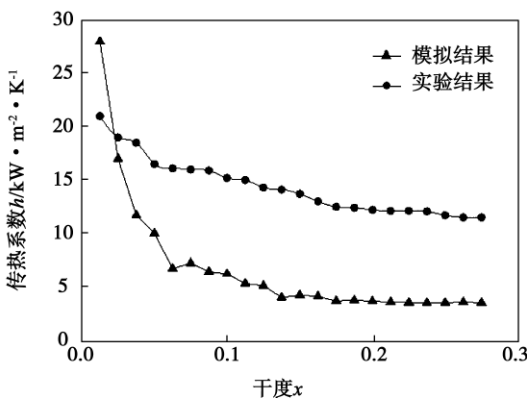


图 5 传热系数和干度的关系

Fig. 5 Relationship between the heat transfer coefficient and dryness

锯齿形细通道内乙醇沸腾工况下,传热系数与干度的关系如图 5 所示,并将模拟结果与文献 [10] 中锯齿形细通道中乙醇沸腾换热的实验研究进行了对比。该文献在双侧加热功率为 56 kW/m^2 的条件下,对质量流率为 $100 \text{ kg}/(\text{m}^2 \cdot \text{s})$ 的乙醇在水力直径为 1.2 mm 的竖直布置细通道内的流动沸腾特性进行了实验研究。所得传热系数与干度关系的实验数据如图 5 所示。可以看出,数值模拟和对比实验的结果都显示出传热系数随系统干度的上升而呈下降的趋势,这种趋势是由细通道沸腾换热的特殊性所决定的。由于通道尺寸很小,所产生气泡的大小与通道尺寸处于同一数量级,出现了诸如泡状流、塞状流等有别于常规通道沸腾的特殊流型,并且由于本模拟的细通道呈锯齿形,某种程度上阻碍了这些

大气泡的运动,使得传热进一步恶化,造成了传热系数的急剧下降。

另外,由图 5 可知,数值模拟的结果明显低于实验结果。造成这一差别的主要原因是实验中所采用的细通道水力直径为 1.2 mm ,小于所模拟的锯齿形细通道宽度 2 mm 宽度。同时,模拟中的一些理想化假设,如壁面粗糙度设为定值等,也可能造成一定的误差。

3 结 论

对竖直布置的锯齿形细通道内乙醇的流动沸腾及换热特性进行了模拟研究,得出结论:

(1) 锯齿形细通道向内侧的突起对由下至上的主流流动起到了较强的扰动作用,由此产生的漂移区改变了过热液体的速度方向,并将其推向主流。成核区与壁面之间还存在着层泡底微层,沿壁面以与主流方向相反的方向流入成核区域,且该作用区内工质的平均流速可达到主流流速的 $5 \sim 10$ 倍。在漂移区和泡底微层的综合作用下,使得锯齿形细通道内侧突起区域附近的换热系数增大,该区域气泡得以快速生长。

(2) 在模拟时间段内,锯齿形细通道系统压差随时间呈上升趋势,并随着细通道内沸腾状态的不同而呈现出变化。

(3) 细通道内沸腾换热所需加热时间短,温度响应迅速,极短的时间内即可达到沸腾状态。核态沸腾过程中气泡数量大,但小气泡会在较短的时间内合并成尺寸与微通道直径相比的大气泡,换热性能随之恶化。

参考文献:

- [1] Ishibashi E, Nishikawa K. Saturated boiling heat transfer in narrow spaces [J]. International Journal of Heat and Mass Transfer, 1969, 12(8): 863-894.
- [2] Tuckerman D B, Pease R F W. High-performance heat sinking for VLSI [J]. IEEE Electron Device Letters, 1981, 2(5): 126-129.
- [3] Fukano T, Kariyasaki A. Characteristics of gas-liquid two-phase flow in a capillary tube [J]. Nuclear Engineering and Design, 1993, 141(1-2): 59-68.
- [4] Mishima K, Hibiki T. Some characteristics of air-water two-phase flow in small diameter vertical tubes [J]. International Journal of Multiphase Flow, 1996, 22(4): 703-712.
- [5] 郭雷, 张树生, 程林. 竖直矩形细通道内水沸腾换热的数值模拟 [J]. 热能动力工程, 2011, 26(1): 31-35. GUO Lei, ZHANG Shu-sheng, CHENG Lin. Numerical simulation of water boiling heat exchange inside a vertical rectangular slim passage [J]. Journal of Engineering for Thermal Energy and Power,

- 2011 26(1):31-35.
- [6] 苏 博,罗小平. 竖直矩形微槽道内的饱和沸腾换热研究[J]. 兰州大学学报(自然科学版) 2008 44(S1):281-284.
SU Bo ,LUO Xiao-ping. Study of saturated boiling heat exchange inside a vertical rectangular microchannel [J]. Journal of Lanzhou University (natural science edition) 2008 44(S1):281-284.
- [7] Bartolomei G G ,Brantov V G ,Molochnikov Y S. An experimental investigation of true volumetric vapor content with subcooled boiling in tubes [J]. Thermal Engineering 1982 29(3):132-135.
- [8] Talebi S ,Abbasi F ,Davilu H. A 2D numerical simulation of sub-cooled flow boiling at low-pressure and low-flow rates [J]. Nuclear Engineering and Design 2009 239:140-146.
- [9] 郭 雷,张树生,陈雅群 等. 竖直狭缝通道内水沸腾换热的气泡动力学研究[J]. 西安交通大学学报 2010 44(11):12-17.
GUO Lei ,ZHANG Shu-sheng ,CHEN Ya-qun ,et al. Dynamic study of the bubbles inside a vertical slim passage during a water boiling heat exchange [J]. Journal of Xi'an Jiaotong University 2010 44(11):12-17.
- [10] Cortina Diaz M ,Schmidt J. Experimental investigation of transient boiling heat transfer in microchannels [J]. International Journal of Heat and Fluid Flow 2007 28(1):95-102.

(丛 敏 编辑)



新技术、新产品

Fr9FB 型燃气轮机的改进及其联合循环装置

据《Gas Turbine World》2011 年 7~8 月刊报道,GE Energy 对其 Fr9FB 型燃气轮机进行了升级和改进,增加了输出功率并提高了效率。

简单循环 50 Hz 9FB 型燃气轮机系列

新型 1500℃ Fr9FB.05 机组计划于 2012 年开始全速和全负荷试验。在 30% 负荷输出功率下能达到 25 mg/kg NO_x 和 25 mg/kg CO 排放。

燃气轮机设计参数	现有 Fr9FB03 机组	Fr9FB.05 机组
推出年份	2002	2014~2015
ISO 基本输出功率	284 000 kW	338 000 kW
LHV 热耗率	9 512 kJ/(kWh)	<9 002 kJ/(kWh)
效率	37.9%	>40.0%
压比	18.1:1	19.7:1
排气质量流量	655 kg/s	745 kg/s
排气温度	642 ℃	623 ℃

50 Hz 联合循环 109FB 型燃气轮机

热态启动时,基于 FB.05 机组的联合循环装置在 30 min 内就能达到 510 MW 全输出功率,并能以每分钟 50 MW 的速度加负荷减少输出功率。在下调到 40% 额定输出功率时能达到 NO_x 和 CO 排放的保证值。

1 对 1 联合循环	现有 109FB.03 装置	109FB.05 装置
推出年份	2002	2014~2015
装置净输出功率	437 184 kW	510 000 kW
LHV 热耗率	6 148 kJ/(kWh)	<5 902 kJ/(kWh)
装置净效率	58.6%	>61.0%
燃气轮机输出功率	284 000 kW	338 000 kW
汽轮机输出功率	162 100 kW	180 000 kW

(吉桂明 摘译)

Engineering for Thermal Energy & Power. - 2012 27(2). - 181 ~ 186

With water serving as the fluid for heat exchange a numerical simulation was performed of the phase-change heat storage of paraffin in a square channel and outside horizontal tubes. Through a reasonable analysis and assumptions, a mathematical model and conditions for definite solutions were established and verified by the test data. With the non-dimensional tube wall temperature Ste number and non-dimensional phase-change material initial temperature G number being introduced, the influence of the Ste and G number on the melting and solidification process of the phase-change material was analyzed with a solid-liquid phase chart of the melting process at various Ste numbers being presented. The research results show that the Ste number has a remarkable influence on the melting and solidification process. The melting duration when $Ste = 0.1875$ is shortened by almost $1/2$ compared with that when $Ste = 0.098$. That when $Ste = 0.277$ is shortened by $1/3$ compared with that when $Ste = 0.1875$. The solidification duration when $Ste = 0.0804$ is shortened by $1/2$ compared with that when $Ste = 0.170$. That when $Ste = 0.259$ is shortened by $1/3$ compared with that when $Ste = 0.170$. However, G number has a relatively small influence on the phase-change process and even the solidification duration can be neglected. **Key words:** phase-change heat storage, mathematical model, melting, solidification

锯齿形细通道内乙醇流动沸腾特性研究 = Study of the Flow Boiling Characteristics of Alcohol in Serrated Slim Passages [刊 汉] CHANG Wei, ZHANG Shu-sheng, GUO Lei (College of Energy Source and Power Engineering, Shandong University, Jinan, China, Post Code: 250061) // Journal of Engineering for Thermal Energy & Power. - 2012 27(2). - 187 ~ 191

By using a numerical simulation method, studied were the flow boiling and heat transfer characteristics of alcohol inside serrated slim passages vertically arranged with a width of 2 mm. The heat and mass transfer process at the phase boundary were controlled by using a UDF (user defined function) programmable method and the bubble growth characteristics and its influence on the system pressure difference and heat exchange coefficient were mainly investigated. The research results show that the initial vaporization nucleation locations inside serrated slim passages tend to be around the inner protrusion points and under the co-action of the drift zone and bubble bottom layer, the mean flow speed of the working medium in the drift zone reaches as high as 5 ~ 10 times of the main stream flow speed, making the bubble growth rate in the zone be quickest and intensifying the heat exchange. The system pressure difference will assume an ascending tendency with the heating time duration and fluctuate in a certain range. The heat exchange coefficient will decrease with an increase of the dryness. The simulation results were analyzed and contrasted with the test data and the influence of the flow pattern and passage geometrical structure on the heat exchange coefficient was also expounded. **Key words:** serrated slim passage, intensified heat transfer, numerical simu-

lation

富氧燃烧条件下煤焦特性研究 = **Study of the Characteristics of Coal Coke Under the Condition of Oxygen-enriched Combustion** [刊, 汉] SUN Shao-zeng, CHEN Hao, MENG Xian-yu, CAO Hua-li (College of Energy Source Science and Engineering, Harbin Institute of Technology, Harbin, China, Post Code: 150001) // Journal of Engineering for Thermal Energy & Power. - 2012 27(2). - 192 ~ 196

With Datong-originated bituminous coal serving as an object of study, on a high temperature carry-over flow simulation reactor, coal coke in an atmosphere for real oxygen-enriched combustion was prepared by using Datong-originated bituminous coal and a horizontal flow flame combustor. An industrial analysis was performed of the coal coke prepared at various residence times with the influence of the residence time on the burn-out rate, fixed carbon and volatile content of the coal coke being discussed. When the residence time is over 94 ms, various parameters of the coal coke are kept unchanged. By using a thermogravimetric analyzer, a combustion test of coal coke was conducted and the influence of various atmospheres at different O_2/CO_2 ratios (20/80, 30/70 and 40/60) on the combustion characteristics of coal coke was discussed. Furthermore, the Coats-Refern method was employed to calculate the activated energy, pre-exponential factor and other dynamic parameters of coal coke. When temperature ranges from 460 to 660 °C and O_2/CO_2 ratio of the background atmosphere reaches 30/70, the activated energy and pre-exponential factor of coal coke attain their maximal values, thus offering a theoretical basis for further studying the combustion reaction of coal coke in the oxygen-enriched combustion atmosphere. **Key words:** oxygen-enriched combustion, coal coke, activated energy

浓缩环对旋流燃烧器 NO_x 生成影响的数值模拟 = **Numerical Study of the Influence of Concentration Rings on the Formation of NO_x Produced By Swirl Burners** [刊, 汉] BI Ming-shu, ZHAO Yao-guang (College of Chemical Industry Machinery, Dalian University of Science and Technology, Dalian, China, Post Code: 116024) // Journal of Engineering for Thermal Energy & Power. - 2012 27(2). - 197 ~ 201

By using the CFD software Fluent, a combustion numerical simulation was performed of a centrally-fed pulverized coal swirl burner. In this connection, the influence of the concentration rings on the formation of NO_x produced by the burner was investigated, the temperature field, oxygen concentration field and NO_x concentration field, including thermal NO_x , fuel NO_x and prompt NO_x , were analyzed when the burner was in its combustion and the NO_x concentration curves along the axial direction at various concentration ring configurations were compared. The simulation results show that the concentration rings can lower the NO_x production capacity of the burner by 100 ~ 200 mg/ m^3 . To adjust both distance of the concentration rings to the port and their intervals can reduce NO_x emissions of